PHILOSOPHICAL TRANSACTIONS OF THE ROYAL SOCIETY A
MATHEMATICAL, PHYSICAL & ENGINEERING SCIENCES

General Discussion: Electronic Emission Spectroscopy of CF $_{4}^{+}$ and SiF$_{4}^{+}$

S. M. Mason and R. P. Tuckett

Phil. Trans. R. Soc. Lond. A 1988 **324**, 289-293
doi: 10.1098/rsta.1988.0018

Phil. Trans. R. Soc. Lond. A **324**, 289–294 (1988)
Printed in Great Britain

General discussion: electronic emission spectroscopy of CF_4^+ and SiF_4^+

By S. M. Mason and R. P. Tuckett
Department of Chemistry, University of Birmingham, P.O. Box 363, *Birmingham B*15 2*TT, U.K.*

with an appendix by R. N. Dixon

We report the observation of electronic emission spectra in the tetrahedral molecular ions CF_4^+ and SiF_4^+. The spectra are observed at a low rotational temperature (less than 30 K) in a crossed molecular-beam – electron-beam apparatus (Carrington & Tuckett 1980). These spectra are especially interesting because the fluorescing states in the two ions lie up to 10 eV above their lowest dissociation channel (to $CF_3^+/SiF_3^+ + F$; see figure 1), and these states might be expected to decay non-radiatively rather than by a radiative channel. The observation of fluorescence decay from highly excited electronic states of these polyatomic ions is therefore a very surprising phenomenon.

Both continuous and discrete bands have been observed for both ions in the visible–ultraviolet region of the electromagnetic spectrum. From photoelectron spectroscopy, the ground and first two excited electronic states ($\tilde{X}$, $\tilde{A}$ and $\tilde{B}$) of CF_4^+ and SiF_4^+ are known to dissociate rapidly, and the continuous bands arise from transitions to these states. These three electronic states arise from electron removal from molecular orbitals in CF_4/SiF_4, which are essentially F 2pπ non-bonding in character. The third and fourth excited electronic states ($\tilde{C}$ and $\tilde{D}$) give vibrational structure in their photoelectron spectra, and hence are bound (figure 1). They arise from electron removal from t_2 and a_1 molecular orbitals in CF_4/SiF_4 that are essentially σ bonding in character. These are the upper states of the bound–free continuous transitions observed in both ions, e.g. CF_4^+ $\tilde{D}$–$\tilde{A}$ at 160 nm, $\tilde{D}$–$\tilde{B}$ at 189 nm, $\tilde{C}$–$\tilde{X}$ at 230 nm (Aarts *et al.* 1987), SiF_4^+ $\tilde{D}$–$\tilde{A}$ at 304 nm (Mason & Tuckett 1987*a*). The discrete bands arise from an allowed transition between the two bound states $\tilde{D}\,^2A_1$–$\tilde{C}\,^2T_2$, and this paper describes this spectrum in CF_4^+ and SiF_4^+ in detail.

Figure 2 shows the discrete band system between 360 and 420 nm obtained with (*a*) electron impact ionization of CF_4 in a molecular beam ($T_{rot} = 25$ K), (*b*) He^+ impact ionization of CF_4 at room temperature (Aarts 1985). The narrowing of the bands at the lower rotational temperature supports the assignment of the emitter as the parent molecular ion of CF_4, and comparison with photoelectron data suggests that the spectrum is caused by vibronic bands of CF_4^+ $\tilde{D}\,^2A_1$–$\tilde{C}\,^2T_2$. A progression is observed only in the ν_1 (a_1) totally symmetric C–F stretching vibration. The absence of any bands involving the ν_2'' (e), ν_3'' (t_2) or ν_4'' (t_2) Jahn–Teller (J.T.) active vibrations shows that there is no J.T. distortion of the $\tilde{C}\,^2T_2$ state from tetrahedral geometry.

Figure 3*a* shows a high-resolution spectrum of the 1_2^0 band at 381 nm obtained in the molecular-beam experiment at 25 K. The spectrum shows a 2:1 doublet that is the spin–orbit splitting of $\tilde{C}\,^2T_2$. Because the higher-wavelength component is the more intense, the $G_{\frac{3}{2}}$ (degeneracy = 4) spin–orbit component of $\tilde{C}\,^2T_2$ has higher energy than the $E_{\frac{5}{2}}$ (degeneracy = 2) component, and hence the spin–orbit splitting is positive. This is a surprising result because

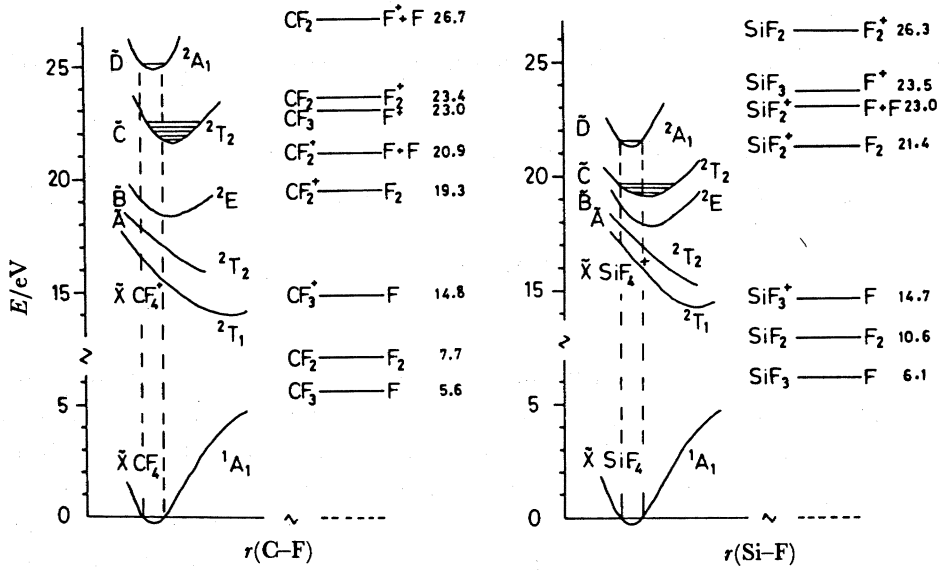

FIGURE 1. Valence ionic states of CF_4 and SiF_4. The energies of the dissociation channels are given in electronvolts.

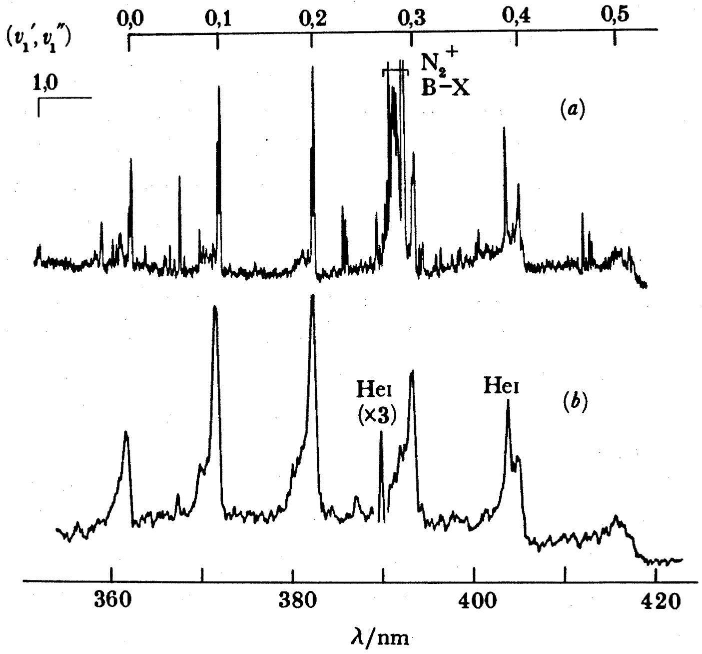

FIGURE 2. (a) The spectrum of CF_4^+ $\tilde{D}$–$\tilde{C}$ resulting from electron-impact ionization of CF_4 at a low rotational temperature; (b) the same spectrum resulting from He^+ impact (1 keV) excitation at a rotational temperature of *ca.* 300 K. The vibrational assignment (v_1', v_1'') is shown.

this state has the $(t_2)^5$ electron configuration, the t_2 orbital is more than half full, and ξ should be negative. An explanation is provided by Professor R. N. Dixon, F.R.S. (Bristol University) in an Appendix to this paper. Figure 3*b* shows a simulation of the band with a model developed by Watson for the rotational structure of a $^2A_1$–$^2T_2$ electronic transition (Watson 1984). The model allows for Coriolis splitting, spin–orbit splitting and J.T. distortion in the $\tilde{C}^2T_2$ state, and

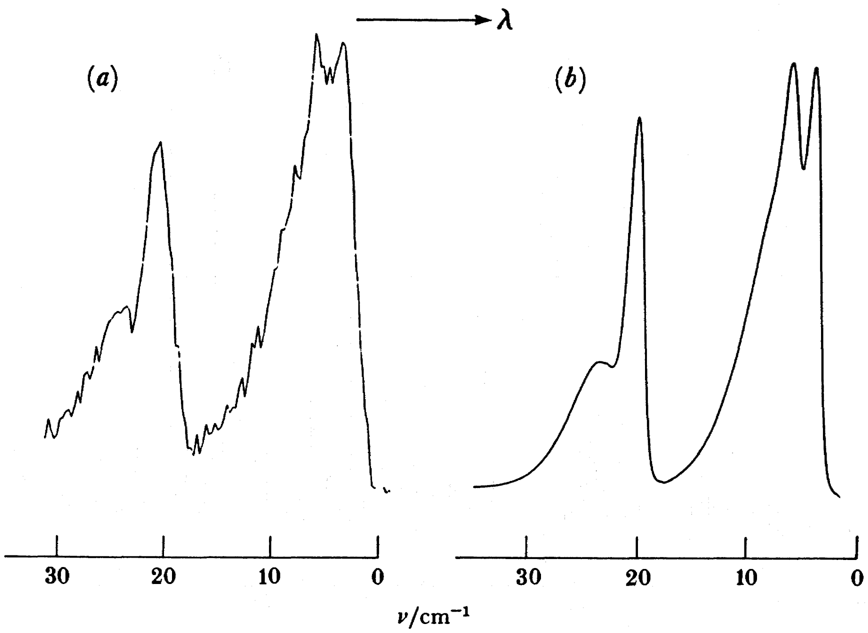

FIGURE 3. (*a*) The 1^0_2 band of CF_4^+ $\tilde{D}$–$\tilde{C}$ at 381 nm recorded at a resolution of 1.5 cm^{-1}; (*b*) shows the simulated spectrum.

can be applied to $\tilde{D}$–$\tilde{C}$ vibronic bands of CF_4^+ or SiF_4^+ that do not involve the J.T. active vibrations (Mason & Tuckett 1987*b*). The main features of the band are determined by two rotational constants, the Coriolis and spin–orbit constant in $\tilde{C}^2T_2$, and the rotational temperature. Estimates of the two rotational constants are made from the intensity distribution of the vibrational bands in the $\tilde{C}$ and $\tilde{D}$ state photoelectron spectra of CF_4. The agreement with experiment is most satisfactory. The positive sign of the spin–orbit splitting is confirmed, and the Coriolis constant in $\tilde{C}^2T_2$ is substantially reduced from its limiting value of $+1$.

Figure 4 shows the analogous $\tilde{D}$–$\tilde{C}$ spectrum in SiF_4^+ around 550 nm recorded at a low rotational temperature in the molecular-beam apparatus (Mason & Tuckett 1987*a*). The spectrum is much more complicated than CF_4^+ $\tilde{D}$–$\tilde{C}$. The allowed progression in ν_1 is observed, but bands involving ν_2'' and ν_4'' are also seen, showing that the $\tilde{C}^2T_2$ state is distorting from T_d symmetry by J.T. distortion. The strong intensity of 4^0_1 suggests that the lower symmetry of $\tilde{C}^2T_2$ is C_{3v}, and the distortion is probably dynamic in nature.

Figure 5 shows high-resolution spectra of the 0^0_0 and the 4^0_1 J.T.-active band at 551 and 564 nm respectively. This is one of the very few observations of a J.T. distortion in a tetrahedral molecule at 'high' resolution (less than 1 cm^{-1}). The spin–orbit splitting of $\tilde{C}^2T_2$ is resolved in both bands, the sign is now uncertain, and its magnitude is quenched in the 4^0_1 band. Our model of the rotational structure can only be applied to the 0^0_0 band, and the simulation of this band is much more difficult than in CF_4^+ for several reasons. Firstly, estimates of the two rotational constants are less accurate than in CF_4^+. Secondly, ΔB is very small and all the constants become highly correlated. Thirdly, the J.T. effect in $\tilde{C}^2T_2$ means that more constants are needed to determine the rotational structure. However, the gross features of the band are reproduced in the simulation (Mason & Tuckett 1987*b*), and as in CF_4^+ the sign of the spin–orbit splitting in SiF_4^+ $\tilde{C}^2T_2$ is confirmed to be positive.

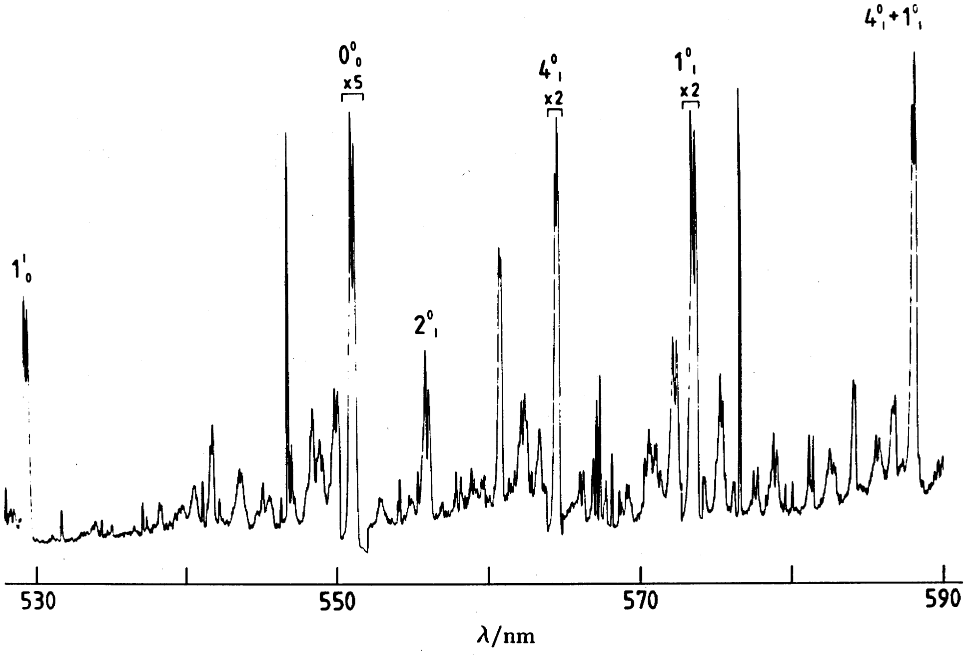

FIGURE 4. The spectrum of SiF_4^+ $\tilde{D}$–$\tilde{C}$ recorded at a low rotational temperature. The resolution is 2.6 cm^{-1}. The very narrow atomic lines are from atomic Si or F.

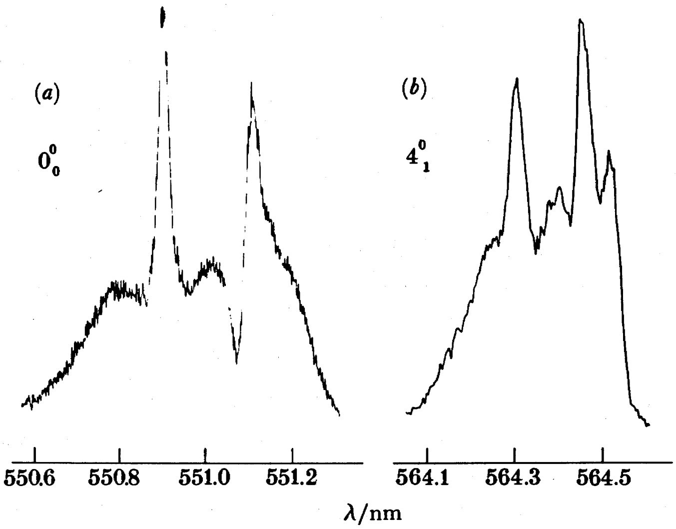

FIGURE 5. (a) The 0^0_0 band of SiF_4^+ $\tilde{D}$–$\tilde{C}$ at 551 nm recorded at a resolution of 0.3 cm^{-1}; (b) the 4^0_1 Jahn–Teller band at 564 nm at a resolution of 0.7 cm^{-1}.

In future experiments we wish to obtain fully rotationally resolved spectra of CF_4^+ and SiF_4^+ $\tilde{D}$–$\tilde{C}$ at Doppler-limited resolution by photographic techniques. Secondly, we wish to understand the dynamics of the decay pathways of the $\tilde{C}$ and $\tilde{D}$ states of CF_4^+/SiF_4^+. Measurements of fluorescence quantum yields and radiative lifetimes will be made by using synchrotron radiation to ionize CF_4/SiF_4 selectively into these excited electronic states of CF_4^+/SiF_4^+. Thirdly, we wish to understand why SiF_4^+ $\tilde{C}\,{}^2T_2$ exhibits dynamic J.T. distortion, whereas CF_4^+ $\tilde{C}$ does not.

REFERENCES

Aarts, J. F. M. 1985 *Chem. Phys. Lett.* **114**, 114.
Aarts, J. F. M., Mason, S. M. & Tuckett, R. P. 1987 *Molec. Phys.* **60**, 761.
Carrington, A. & Tuckett, R. P. 1980 *Chem. Phys. Lett.* **74**, 19.
Mason, S. M. & Tuckett, R. P. 1987*a* *Molec. Phys.* **60**, 771.
Mason, S. M. & Tuckett, R. P. 1987*b* *Molec. Phys.* (In the press.)
Watson, J. K. G. 1984 *J. molec. Spectrosc.* **107**, 124.

APPENDIX. THE SIGN OF THE SPIN–ORBIT COUPLING CONSTANT IN $(t_2)^5\,{}^2T_2$ STATES OF AX_4^+ IONS

By R. N. DIXON, F.R.S.

*School of Chemistry, University of Bristol, Cantock's Close, Bristol BS*8 1*TS, U.K.*

The spin–orbit splitting in orbitally degenerate systems with one open shell usually conforms to Hund's third rule: that is, the splitting is regular for a less than half-filled shell, and inverted for a more than half-filled shell. The $\tilde{C}\,{}^2T_2$ states of CF_4^+ and SiF_4^+ reported by Mason & Tuckett violate this expectation. We show below how this may occur in AX_4^+ ions where the dominant atomic spin-orbit coupling arises from motion around the X atoms.

For $(t_2)^5\,{}^2T_2$ states we consider only the spin–orbit coupling matrix elements within the t_2 shell, and use a basis of symmetry-adapted components which transform as translations parallel to the three cubic axes (Dixon *et al.* 1971). There are three types of t_2 basis function involving atomic p-orbitals, one localized on A and two on X_4:

$$\left.\begin{aligned} 1t_{2x} &= x_A, \\ 1t_{2y} &= y_A, \\ 1t_{2z} &= z_A. \end{aligned}\right\} \tag{A 1}$$

$$\left.\begin{aligned} 2t_{2x} &= \tfrac{1}{2}(x_1+x_2+x_3+x_4), \\ 2t_{2y} &= \tfrac{1}{2}(y_1+y_2+y_3+y_4), \\ 2t_{2z} &= \tfrac{1}{2}(z_1+z_2+z_3+z_4). \end{aligned}\right\} \tag{A 2}$$

$$\left.\begin{aligned} 3t_{2x} &= \tfrac{1}{2\sqrt{2}}(y_1-y_2+y_3-y_4+z_1+z_2-z_3-z_4), \\ 3t_{2y} &= \tfrac{1}{2\sqrt{2}}(x_1-x_2+x_3-x_4+z_1-z_2-z_3+z_4), \\ 3t_{2z} &= \tfrac{1}{2\sqrt{2}}(x_1+x_2-x_3-x_4+y_1-y_2-y_3+y_4). \end{aligned}\right\} \tag{A 3}$$

Note that for $3t_2$ the p-orbitals at each atomic centre can be combined into a single p-orbital directed at 90° to the translation axis of the basis function (see figure A 1), whereas it is parallel to this axis for $1t_2$ and $2t_2$.

In calculating spin–orbit matrix elements we shall only include integrals involving two atomic orbitals of the same atom. It is then sufficient to use a pseudo one-electron hamiltonian of the following form

$$H'_{\text{S-O}} = \sum_{i=1}^{5} \sum_{k} \xi_k\, l_k(i) \cdot s(i), \tag{A 4}$$